Advanced International Journal for Research (AIJFR)
E-ISSN: 3048-7641 ● Website: www.aijfr.com ● Email: editor@aijfr.com

Hypersonic Simulations for Surface Heat Transfer Measurements on Orion Crew Exploration Vehicle

Arun Prathap[1], Rishab M. Chitgopekar[2], Sai K. Ullal[3], Raunak G. Mahenderkar[4], Deepanshu K. Punjabi[5], Jayahar Sivasubramanian[6]

[1,2,3,4,5,6] Department of Aerospace and Automotive Engineering, M. S. Ramaiah University of Applied Sciences, Bangalore, India

Abstract
Computational Fluid Dynamics (CFD) simulations using the Stanford University Unstructured (SU2) solver were employed to investigate the impact of hypersonic flow over Orion Crew Exploration Vehicle (CEV) during atmospheric entry. The study looked at two scenarios, the first scenario included modelling flow over the body at two different Mach numbers using RANS equations, and the second looked at the impact of non-equilibrium flows on the body.

Keywords: CFD, Aerodynamic Heating, Shock Waves, Hypersonic Flight, Crew Exploration Vehicle.

1. Introduction

The phenomenon of atmospheric entry unfolds when a body in outer space enters the atmosphere of a planet and temperature rises. The body might be natural, like an asteroid, or man-made, like a satellite or re-entry vehicle. Because of its rapid velocity, the body in the atmospheric entry encounters extremely high temperatures, with Mach values exceeding 20. The heating effect is caused by the body attempting to shed its high kinetic energy by converting it to heat energy [1,2,3].

The fundamental design goal of a spacecraft's atmospheric entry is to dissipate the energy of a hypersonic spacecraft as it enters an atmosphere, slowing down equipment, cargo, or any passengers and landing at zero velocity near a desired location on the surface while keeping stresses on the spacecraft and any passengers within acceptable limits. Propulsive or aerodynamic measures can be used to accomplish this. It is critical to design the re-entry body to minimize surface heating, since this is critical in ensuring that the cargo or payload onboard is not harmed [4]. This necessitates a thorough grasp of flow mechanics as well as an in-depth comprehension of hypersonic flow phenomena. We can complete most of these jobs using powerful and open-source CFD tools, such as SU2.

2. Literature Review and Objective

The hypersonic flow regime is where flow velocity is greater than 5 times the speed of sound, usually starting at Mach 5 or above [3]. Since specific physical changes in the airflow occur at different speeds, the precise Mach number at which a vessel can be claimed to fly at hypersonic speed varies. These effects

cumulatively become significant around Mach 5-10. In hypersonic flows the shock distance between the body and the shock wave is comparatively lower than supersonic regime. The flow is fast, and the kinetic energy is high. Frictional forces cause the air to slow down and create heat. This is known as aerodynamic heating. This causes extremely high temperatures behind the shock and at the body's surface. A blunt body is typically employed for atmospheric entry because it causes the shock to be removed from the body. This greatly decreases temperatures near the body's surface because there is a layer of air between the shock and the body that functions as a convection zone for the air molecules to absorb and transfer heat away from the body [4].

The perfect gas model assumes that the gas molecules are indistinguishable, tiny, and hard spheres, that there are no energy losses in motion or during collisions between molecules, and that the average distance between molecules is substantially greater than the size of the molecules. However, at high temperatures, the gas molecules dissociate and ionize. The specific heat of the gas is affected by pressure and temperature. As a result, gas cannot be considered to be calorically perfect, implying that ideal gases cannot be employed. Molecular collisions cause vibrational and chemical changes at high temperatures. However, for the modifications to occur, a significant number of collisions must occur, which takes time. In equilibrium systems, it is assumed that the gas has adequate time for collisions to occur and that the system's attributes remain constant at a set pressure and temperature. RANS solver with ideal gas model is used to simulate equilibrium flow conditions [5].

The non-equilibrium flow area is a region where the molecules and particles of the system are in a non-equilibrium phase between the time it takes for the new equilibrium phase. After a rapid change in pressure and temperature, the vibrational and chemical characteristics of a non-equilibrium system alter. Collisions between molecules are required for the system's constituents to acquire this new equilibrium state, which takes time. In order to capture the non-equilibrium effects NEMO solver paired with AIR_5 is used with mutation++ library [6,7].

3. Governing Equations

For the case considered, the Navier-Stokes equations and SU2-NEMO governing equations are the ones that have been used. SU2 solves the compressible Navier-Stokes equations expressed in differential form as:

$$\mathcal{R}(U) = \frac{\partial U}{\partial t} + \nabla \cdot \bar{F}^c(U) - \nabla \cdot \bar{F}^v(U, \nabla U) - S = 0 \tag{1}$$

The Navier–Stokes equations are extended for reacting flows in thermochemical nonequilibrium to simulate continuum hypersonic flows in SU2-NEMO [7]. This is a set of connected nonlinear partial differential equations in conservation form.

$$\mathrm{R}(\mathrm{U}, \nabla \mathrm{U}) = \frac{\partial \mathrm{U}}{\partial t} + \nabla \cdot \mathrm{F}^c(\mathrm{U}) - \nabla \cdot \mathrm{F}^v(\mathrm{U}, \nabla \mathrm{U}) - \mathrm{Q}(\mathrm{U}) = 0 \tag{2}$$

The governing equations for heat flux that are incorporated in the SU2 code are given below,

$$\frac{\partial T}{\partial \eta} = \frac{T_{w+1} - T_w}{d_{ij}} \quad , \quad k = \frac{\mu c_P}{\mathrm{Pr}} \quad , \quad q_w = -k\frac{\partial T}{\partial \eta} \tag{3}$$

During high-speed flows, thermal nonequilibrium happens when a gas's internal energy cannot be described by a single temperature, and chemical nonequilibrium occurs when its chemical state does not match chemical equilibrium criteria. As a result, non-equilibrium thermal and chemical zones occur. This is due to the fact that much of the gas's kinetic energy is converted to random translational motion when it passes through the bow shock wave. Collisions transform translational energy into rotational, vibrational, electronic, and chemical energy. This energy transfer necessitates a certain number of collisions, during which the gas travels to a new place with potentially changing temperature and density. The energy carried by polyatomic molecules in a gas-phase species is divided into translational, rotational, vibrational, and electronic degrees of freedom. The energy of each mode is quantized, and the allowable energy levels are specified by the eigenstates of the time-independent Schrödinger equation. [12]

To account for differences in the number of collisions necessary to attain equilibrium, SU2-NEMO adopts a two-temperature model in which the translational–rotational energy modes and vibrational–electronic energy modes are tracked at separate temperatures. The translational and rotational energy modes, as well as the vibrational and electronic modes, are thought to be in balance in this two-temperature model, however the two are not always in equilibrium.
The total energy and vibrational–electronic energy per unit volume in SU2 are be represented as:

$$\rho e = \sum_s \rho_s \left(e_s^{tr} + e_s^{rot} + e_s^{vib} + e_s^{el} + e_s^{\circ} + \frac{1}{2}\mathbf{u}^T\mathbf{u} \right) \tag{4}$$

$$\rho e^{ve} = \sum_s \rho_s \left(e_s^{vib} + e_s^{el} \right) \tag{5}$$

When atmospheric entry speeds surpass Mach 20. The environment behind a typical shock in front of the entry module will be substantially different from the atmosphere before the shock in the higher regions of the atmosphere. According to gas dynamics from [13], the normal shock strength increases as the free stream velocity increases. An ideal gas model would vastly overestimate surface temperatures because flow continuity breaks at high elevations when air density is low.

4. Simulation Setup and Numerical Methods

A. SU2 Software

Stanford University Unstructured, abbreviated as SU2. It is an open-source CFD solver using finite element or finite volume. It is developed in the C++ programming language and includes Python scripts

that allow for the automation of numerous operations and increase usability. It can solve non-equilibrium flow problems using the SU2-NEMO solver. Mutation++ allows you to mimic a large range of various gas compositions. This library allows us to simulate non-equilibrium flows at double the pace of the default non-equilibrium resources provided by SU2. As a result, it was widely employed in non-equilibrium flow simulations [7,8].

B. Assumptions

Two distinct instances are addressed in the simulations. The first is when the re-entry module is well into the atmosphere and the Knudsen number, defined as the ratio of the mean free path to the characteristic length, is within the range necessary to assume continuous flow. Because the software utilized is SU2, it is assumed that the flow's continuum is still valid in the second situation when the re-entry module is high in the atmosphere and the Knudsen number is very low and continuum flow is no longer acceptable and the flow must be deemed rarefied.

C. Orion geometry

The most common geometries for entering planetary atmospheres are blunt body kinds. This arrangement facilitates the production of a disconnected shock, which is desired since it not only shields the body from excessive aerodynamic heating, but also creates a significant amount of aerodynamic drag, slowing the spacecraft down from orbital or interplanetary speeds. Orion (CEV) is a partly reusable crewed spacecraft developed by NASA for the Artemis programme. The design of the CEV is similar to that of Apollo, with a spherical section heat shield shielding a truncated-cone-shaped crew compartment, but it is much broader. The CEV's newest design iteration has a maximum diameter of 5 meters. The geometry was generated in Catia V5R19 for the simulation using the dimensions indicated below.

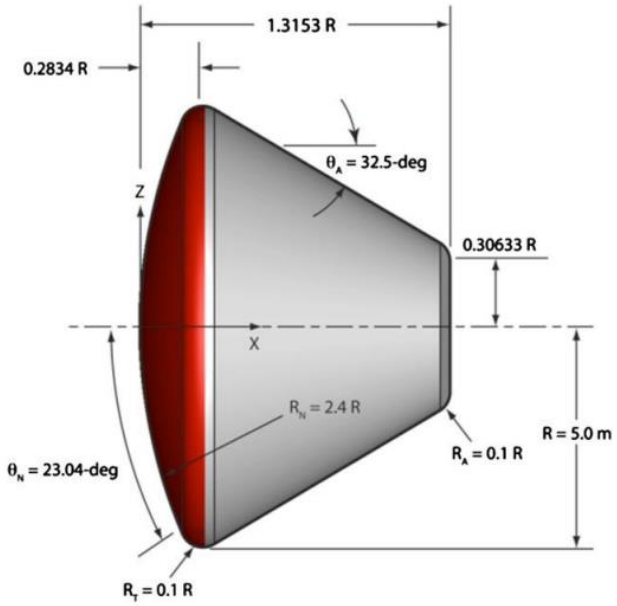

Fig 1. Orion CEV module dimensions

D. Computational grid

Gmsh, an open-source software, was used to construct all computational grids. Gmsh generates cells using a transfinite approach, which allows for greater control over the quantity of grid points added to a surface as well as their distribution. An inflation layer was constructed along the surface to capture the surface boundary layers and flow patterns. A refinement zone using structured mesh is constructed around the blunt nose to collect shock details. The inflation layer and refinement zone will work together to keep the y-plus as low as feasible. The three types of meshes developed for simulation were structured, unstructured, and refinement plus inflation layer. Farfield and Wall were designated as boundary conditions.

E. Problem statement

Two Mach values were used in the CFD simulations on the Orion module: Mach 7.8 and Mach 26.7. For each of these Mach values, RANS equations were used to simulate chemically non-reacting flow, while SU2's NEMO-solver was used to simulate chemically reacting non-equilibrium flow. The Mach 26.7 example is studied at a high altitude, seeking to reproduce the first atmospheric entry phase, whereas the Mach 7.8 instance studies hypersonic flow over the body after it has plummeted well into the atmosphere. The most essential criterion is heat flow, which was compared using RANS for both scenarios. Due to the massive hardware required to produce precise findings, heat flux for the non-equilibrium flow was not computed using the NEMO-solver [7]. Furthermore, because the temperatures measured were simply impractical owing to the assumption of continuum flow for the Mach 26.7 example, they were not included in the research.

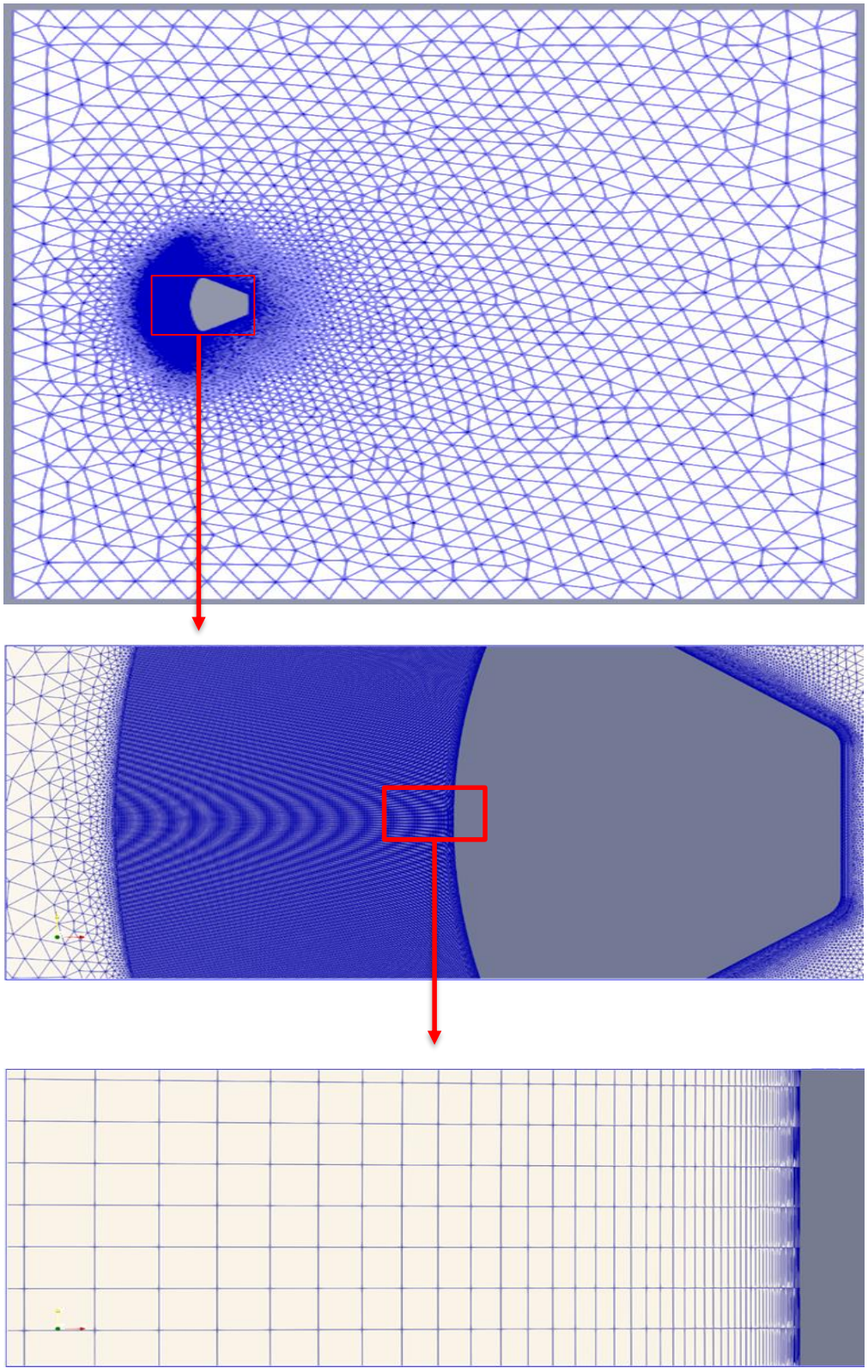

Fig 2. Computational grid with refinement zone and inflation layer a) Whole domain, b) Refinement zone, c) Inflation layer.

F. Initial Conditions and solver settings

Table 1. Initial conditions and solver settings

Flow conditions		
Angle of attack	0 degrees	
Reynolds number	10E8	10E4
Mach number	7.8	26.7
Freestream Pressure	8670 Pa	0.32 Pa
Freestream temperature	74.1 K	195 K
Wall temperature	300 K	800 K
Knudson number	0.01	0.03
Turbulence model	Spallart -Almaras	

5. Results and Discussion

A. Pressure Distribution Comparison

The Mach 7.8 flow case is used to compare the pressures of each grid. Figure 3 shows that the highest-pressure values recorded from all three grids are within 2% of the case's predicted isotropic pressure value, which is shown by a grey circle on the y-axis. This demonstrates that the pressure values for the considered instance are not affected by the grid.

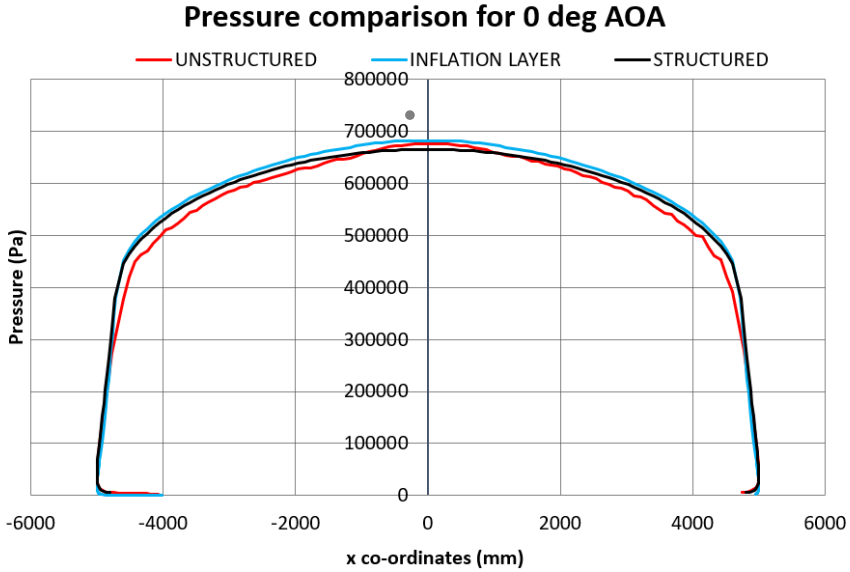

B. Heat Flux Distribution

To correctly assess heat fluxes, an extremely fine grid must be employed in the simulation, with over 70% of the cells concentrated near the wall, in order to compute the flow. At the stagnation point, the maximum heat flow occurs [10].

Table 2. Peak heat flux comparison

Peak heat flux (W/m^2)	Mach number
32,125	26.7
21,752	7.8

Fig 3. Pressure comparison plot (along the body surface)

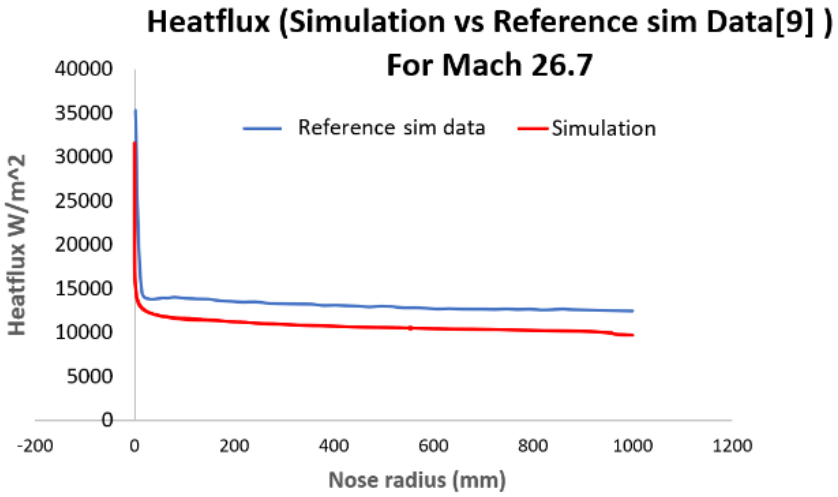

Fig 4. Comparison of results obtained in the simulation conducted with the results from a reference paper performing simulations for a comparable case.[9]

C. RANS VS NEMO

The Mach and temperature contours are compared between the RANS solver, which employs the ideal gas equation, and the NEMO solver, which simulates the gas's non-equilibrium reactive effects at high temperatures. The shock is visible as a single line in front of the body and along the flow in the RANS result, and the wake is shown extremely clearly with clear differences between the areas of the flow downstream of the shock.

The shock is visible as a single line in front of the body and along the flow in the RANS result, and the wake is shown extremely clearly with clear differences between the areas of the flow downstream of the shock. The NEMO result in Figure 6 shows that the shock does not appear as a single line and that the

flow downstream of the shock in the wake region seems scattered or more spread out than the RANS result. This is the zone of non-equilibrium flow [11,12].

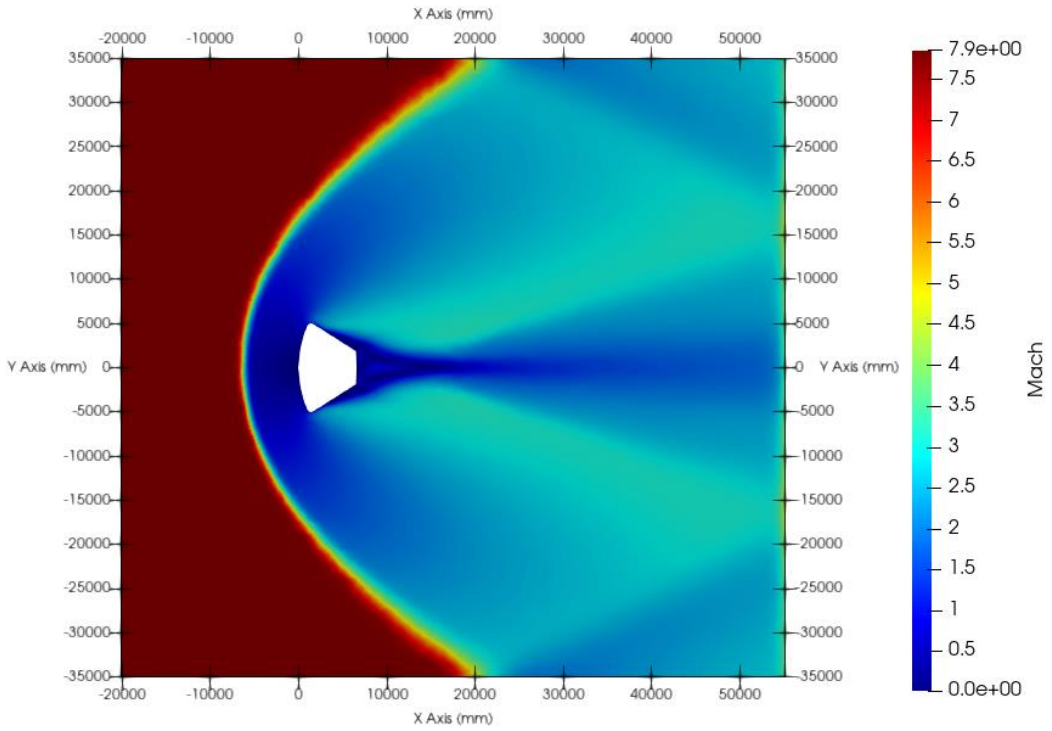

Fig 5. Mach contour for Mach 7.8 using the ideal gas model (RANS**)**

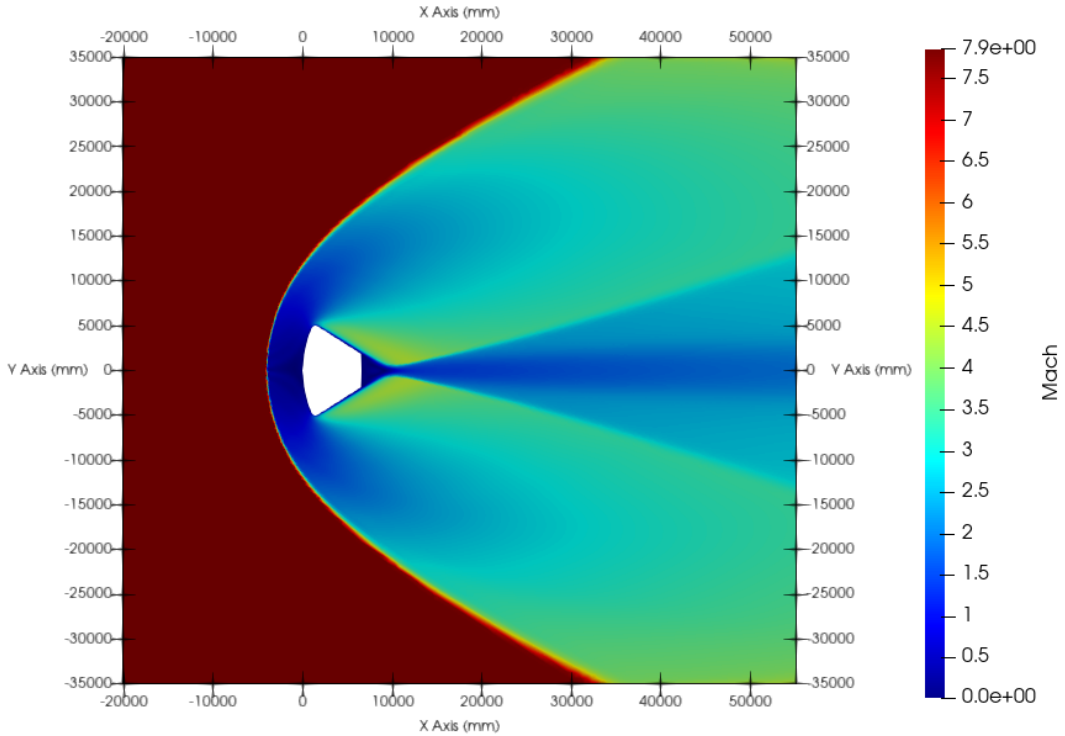

Fig 6. Mach contour for Mach 7.8 using the SU2-NEMO equations

When we compare the peak temperature at the stagnation point (data shown in Table 3), we see that the ideal gas model considerably overpredicts the temperatures throughout a shock wave at high temperatures since it only considers the molecule to have translational energy. The temperatures anticipated in the non-equilibrium situation are substantially lower, leading to the conclusion that the temperatures are predicted more precisely using the NEMO solver, which takes non-equilibrium flow physics into account.

Peak temperature (in K)	**Governing equations**
4051	RANS
2173	NEMO Navier-Stokes

Table 3. Temperature comparison between RANS and NEMO for Mach 7.8

6. Conclusions

In this work the equilibrium and non-equilibrium flow effects for high-speed flows over the Orion CEV re-entry vehicle is investigated. Various parameters were studied, such as pressure distribution along the surface of the vehicle, heat flux distribution along the surface for different Mach numbers and comparing RANS equations with non-equilibrium flow equations. It was established that heat flux and pressure are at their peak value at the stagnation point. A grid independent study was conducted for pressure calculations, and it was determined that to obtain accurate heat flux values, a highly refined and concentrated grid is needed. The heat flux data was also compared that conducted a similar simulation over the Orion CEV module, wherein the difference of values were found to be within 5 percent. Following this a comparison between the RANS solver and NEMO solver was carried out from which it was established that the ideal gas model over predicts temperatures with the peak temperature of the former being 4051K and the latter being 2173K. As a result, it was concluded that the NEMO-solver using Mutation++ predicts the temperatures much more accurately as well as giving a much more realistic representation of the Mach contour, due to the consideration of non-equilibrium flow effects.

References

1. Pappachan, Joseph, (2015) "*Numerical simulation of Orion CEV re-entry vehicle at low altitude"*. Dissertation, Indian Institute of Technology Hyderabad, 2015.
2. Hirschel, Ernst Heinrich, and Claus Weiland, (2009) "*Selected aerothermodynamic design problems of hypersonic flight vehicles"*. Vol. 229. Springer Science & Business Media, https://doi.org/10.1007/978-3-540-89974-7, 2009.
3. Anderson, John David, (2000) "*Hypersonic and high temperature gas dynamics"*, AIAA, 2000.
4. Papadopoulou, Ermioni, (2014) "*Numerical Simulations of the Apollo 4 Re-entry Trajectory"*. Master Thesis, Ecole Polytechnique, 2014.
5. Mehta, R. C. (2008) "*Computations of Flow Field over Apollo and OREX Reentry Modules at High Speed*." *INDIAN J. ENG. MATER. SCI.*, Vol. 15, Issue 6, 2008.
6. Versteeg, Henk Kaarle, and Weeratunge Malalasekera. (2007) "*An introduction to computational fluid dynamics: the finite volume method"*. Pearson Education, 2007.

7. Maier, Walter T., Needels, Jacob T., Garbacz, Catarina., Morgado, Fabio., Alonso, Juan J., and Fossati, Marco. (2021) "*SU2-NEMO: An open-source framework for high-Mach nonequilibrium multi-species flows." Aerospace*, 8(7), 2021.
8. Moyer, C. B., and Rindal, R. A., (1968) "*An Analysis of the Coupled Chemically Reacting Boundary Layer and Charring Ablator – Part II. Finite Difference Solution for the In-Depth Response of Charring Materials Considering Surface Chemical and Energy Bal*ances", NASA CR-1061, 1968.
9. Patel, Rakeshkumar K., and K. Venkatasubbaiah., (2013) "*Numerical simulation of the Orion CEV reentry vehicle*." *Journal of Aerospace Engineering*, 28(2), 2013.
10. Sanjeev Kumar Manjhi and Rakesh Kumar., (2018) "*Stagnation point transient heat flux measurement analysis from coaxial thermocouples*", Experimental Heat Transfer, 31(5), 405–424. https://doi.org/10.1080/08916152.2018.1431738.
11. Yates, J.T.; Johnson, J.K., (2007) "*Molecular Physical Chemistry for Engineers"*, 1st ed.; University Science Books: Sausalito, CA, USA, 2007.
12. Anderson, J. D., (2004). "*Modern compressible flow with historical perspective"*, McGraw-Hill, Singapore.